substances including solid-state materials. Such ideas can relate two-dimensional aromaticity in planar aromatic hydrocarbons such as benzene to three-dimensional aromaticity in deltahedral boranes such as $B_nH_n^{2-}$ ($6 \leq n \leq 12$). In addition, topological ideas have been essential for the development of the chemistry of bare gas-phase post-transition-element clusters by suggesting key experiments. In the case of infinite solid-state structures, ideas derived from topology not only relate chemical structure and bonding to superconductivity as discussed in this Account but also provide the first viable approach to chemical bonding in icosahedral quasicrystals.[86] These diverse examples clearly demonstrate the wide applicability of mathematical methods to structure and bonding in inorganic chemistry.

I am indebted to the U.S. Office of Naval Research for financial support of this work during the period 1984–1988 when many of the ideas outlined in this Account were developed. This Account is based on the award lecture for the 1991 American Chemical Society award in inorganic chemistry sponsored by Monsanto Company presented at the 201st National Meeting of the American Chemical Society, Spring 1991, in Atlanta, GA.

(86) King, R. B. *Inorg. Chim. Acta* **1991**, *181*, 217.

Dynamic Monte Carlo Simulations of Surface-Rate Processes

H. CHUAN KANG

Department of Chemistry, National University of Singapore, Singapore 0511, Singapore

W. HENRY WEINBERG*

Department of Chemical Engineering, University of California—Santa Barbara, Santa Barbara, California 93106-5850

Received September 24, 1991 (Revised Manuscript Received February 28, 1992)

Monte Carlo methods have been widely used in many areas of chemical physics.[1,2] In recent years they have been employed to study various equilibrium and dynamic problems in surface science.[3-12] When Monte Carlo methods are used in studying equilibrium phenomena, many replicas of the system of interest are generated according to some sampling algorithm. Although consideration must be given to finite-size effects, rather accurate results may be obtained if a sufficient number of replicas of the system are generated. In the case of dynamic phenomena, however, an additional basic issue must be addressed to ensure that the Monte Carlo simulations yield correct results. The correspondence between each step in a Monte Carlo simulation and real time must be established. In the section Dynamic Monte Carlo Simulations, we review some work[13,14] in which this correspondence has been studied and discuss the dynamical interpretation of Monte Carlo simulations. In the section Applications, we review two applications of dynamic Monte Carlo simulations, one concerning surface diffusion and the other concerning the compensation effect in surface reactions. In the first application the importance of the appropriate choice of transition probabilities is demonstrated. In the second application we show how Monte Carlo simulations can provide useful results for a reacting lattice-gas system.

Dynamic Monte Carlo Simulations

We begin this section by describing a simple algorithm for a dynamic Monte Carlo simulation of the surface diffusion of atoms or molecules adsorbed on a crystal surface. In this algorithm for surface diffusion, particles (atoms or molecules) hop from one site to another on a lattice which has a coordination number dictated by the symmetry of the crystal surface. The lattice is initially populated randomly at some specified

H. Chuan Kang was born in Malaysia on November 28, 1959. He received a B.S. degree in chemical engineering in 1983 from Yale University and a Ph.D. degree, also in chemical engineering, from the California Institute of Technology in 1989. He was a postdoctoral fellow in the Department of Chemistry and the Ames Laboratory of Iowa State University until he assumed his present position of Assistant Professor of Chemistry at the National University of Singapore in 1991. His research interests are in the area of numerical simulations of surface phenomena.

W. Henry Weinberg was born in South Carolina on December 5, 1944. He received a B.S. degree in chemical engineering in 1966 from the University of South Carolina and a Ph.D. degree in chemical engineering from the University of California, Berkeley, in 1970. After a postdoctoral year in physical chemistry at Cambridge University, he joined the faculty of the California Institute of Technology in 1972. In 1989 he assumed his present position as Professor of Chemical and Nuclear Engineering and Professor of Chemistry at the University of California, Santa Barbara. He has been the recipient of numerous awards and prizes during the past 20 years, most recently the 1991 ACS award in surface or colloidal chemistry. This paper is based on his award address at the ACS meeting in Atlanta in April 1991. His research interests include experimental and numerical studies of the chemistry and physics of transition metal and semiconductor surfaces.

(1) *Monte Carlo Methods in Statistical Physics*; Binder, K., Ed.; Topics in Current Physics, Vol. 7, Springer-Verlag: Berlin, 1986.
(2) *Applications of the Monte Carlo Method in Statistical Physics*; Binder, K., Ed.; Topics in Current Physics, Vol. 36; Springer-Verlag: Berlin, 1987.
(3) Hood; E. S.; Toby, B. H.; Weinberg, W. H. *Phys. Rev. Lett.* **1985**, *55*, 2437–2440.
(4) Silverberg, M.; Ben-Shaul, A. *J. Chem. Phys* **1985**, *83*, 6501–6513.
(5) Silverberg, M.; Ben-Shaul, A. *Chem. Phys. Lett.* **1987**, *134*, 491–496.
(6) Silverberg, M.; Ben-Shaul, A. *Surf. Sci.* **1989**, *214*, 17–43.
(7) Araya, P.; Porod, W.; Sant, R.; Wolf, E. E. *Surf. Sci.* **1989**, *208*, L80–L90.
(8) Dumont, M.; Poriaux, M.; Dagonnier, R. *Surf. Sci.* **1986**, *169*, L307–L310.
(9) Sales, J. L.; Zgrablich, G. *Phys. Rev.* **1987**, *B35*, 9520–9528.
(10) Sales, J. L.; Zgrablich, G. *Surf. Sci.* **1987**, *187*, 1–20.
(11) Gupta, D.; Hirtzel, C. S. *Chem. Phys. Lett.* **1988**, *149*, 527–533.
(12) Gupta, D.; Hirtzel, C. S. *Surf. Sci.* **1989**, *210*, 322–338.
(13) Kang, H. C.; Weinberg, W. H. *J. Chem. Phys.* **1989**, *90*, 2824–2830.
(14) Fichthorn, K. A.; Weinberg, W. H. *J. Chem. Phys.* **1991**, *25*, 1090–1096.

0001-4842/92/0125-0253$03.00/0

fractional coverage. This random occupation of the lattice sites corresponds either to a configuration of adsorbed molecules at a sufficiently high surface temperature that the lateral interaction energies are much smaller than k_BT, or to a configuration of molecules adsorbed randomly on a surface at such a low temperature that no surface diffusion occurs.

The lattice-gas configuration is updated as follows. A particle is chosen at random, and then one of the z nearest-neighbor sites is chosen randomly. If this latter site is occupied by another lattice-gas particle, the attempted hop is not successful, and the procedure is repeated. If, however, the site is vacant, the particle hops into it from its original site with a probability $\omega(c_i,c_f)$, where c_i and c_f denote the initial and final configurations of the lattice gas. Generally, the probability of hopping $\omega(c_i,c_f)$ of an adsorbed molecule depends upon its neighbors because of lateral interactions. For each attempted hop, time is incremented by one Monte Carlo step. This corresponds to some unit of real time, τ/N, where N is the total number of lattice-gas particles; and each particle is excited once by the heat bath in each time interval τ. This procedure is reiterated.

We have described above how a Monte Carlo simulation for surface diffusion may be performed. Extension of the algorithm to include desorption, adsorption, or reaction is simple. Each of these microscopic processes can be treated in an analogous manner as for surface diffusion. In the case of desorption, for example, a particle that is picked has a probability of desorption given by $\omega(c_i,c_f)$, where c_i and c_f in this case denote the configuration of the lattice with the chosen particle in its original site and the configuration of the lattice with the chosen particle desorbed into the gas phase, respectively. Thus, in general, the lattice-gas configuration in a simulation can change as a result of a particle hopping from one site to a neighboring site, a particle desorbing into the gas phase, a particle adsorbing from the gas phase into a vacant site, or two particles reacting and desorbing into the gas phase. It should be apparent that the efficiency of such algorithms is rather strongly dependent upon the transition probabilities $\omega(c_i,c_f)$ for the various microscopic events. If these transition probabilities are small, there will be many attempts at a transition for each successful change in the lattice-gas configuration. In the case of surface diffusion, for instance, many unsuccessful attempts at hopping will occur for each successful hop. This is clearly not a desirable situation.

Fortunately, Monte Carlo simulations that avoid this problem can be implemented.[15] Rather than particles being picked at random, as in the above algorithm, a list of the possible hops for the current lattice-gas configuration is constructed. Corresponding to each of these possible hops is a probability of success. The hop which actually occurs is chosen according to its probability of success, and the configuration is updated. This approach ensures that each iteration of the simulation results in a change in the configuration. Two features of this approach should be noted.

First, a list of all possible events must be made, and this list must be updated after each event. Depending upon the system, this list can be rather long. Therefore, in implementation of a Monte Carlo simulation, this fact should be taken into consideration. If events occur rapidly, that is, with large transition probabilities $\omega(c_i,c_f)$, then it is advantageous to simulate the system as described earlier. Since the configuration of the system will evolve toward lower energy, the transition probabilities will generally decrease during the course of a simulation. Hence, it might be advantageous to combine the two algorithmic approaches described above such that initially, when the transition probabilities $\omega(c_i,c_f)$ are high, the first approach is used, and later, when the configurational changes slow down, the second approach is brought into play.

Second, because the events that actually occur are chosen according to their probability of success, each Monte Carlo step does not correspond to a constant time increment, in contrast to the first algorithm that was described. Each Monte Carlo step corresponds to a time increment which must be computed by an appropriate weighting of all the events that could possibly occur at that step. The procedure to determine the correct time increment has been previously established using the theory of the Poisson process.[14] Here, we shall derive equivalent results from a slight different point of view and, specifically, for nonstationary processes.

Consider an ensemble of n_0 configurations for which the average rate of occurrence of a transition is equal to r. Then the number n of configurations in the ensemble in which a transition has not occurred after time t is given by $n_0 \exp(-rt)$. Therefore, the number of configurations dn for which a transition occurs in the interval of time from t to $t + dt$ is equal to $rn_0 \exp(-rt)\, dt$. From this distribution of waiting times, the average waiting time for a transition is given by $n_0^{-1}\int_0^\infty trn_0 \exp(-rt)\, dt$, which is equal to r^{-1}. Hence, the time increment Δt between events can easily be related to the rate of occurrence of transitions, which can, in turn, be calculated from the microscopic transition probabilities, i.e., $\Delta t = r^{-1} = \langle\langle \omega(c_i,c_f)/\tau \rangle\rangle^{-1}$. Here, $\langle\langle\ \rangle\rangle$ indicates that the average is taken over all final configurations c_f for each initial configuration c_i, and also over all initial configurations c_i that occur in the ensemble.

Thus, a dynamic Monte Carlo simulation can be performed in the following fashion. Generate a configuration defined by some macroscopic parameters, for example, a specified fractional coverage and a spatial distribution corresponding to some specified initial temperature. Then make a list of all possible transitions and compute the average rate for a transition. A transition is then picked according to its probability, and the lattice configuration is updated. This process is reiterated until a sufficiently long sequence of configurations has been obtained. In this way, a trajectory in configuration space is generated. By repetition of the process many times, each time starting with a different configuration specified by the same macroscopic parameters (temperature and fractional coverages, for example), an ensemble of trajectories is generated. Corresponding to each Monte Carlo step in this ensemble is a time increment which is calculated by taking the reciprocal of the average, over the ensemble, of the transition rate. Such an algorithm for a system approaching equilibrium through adsorption and desorption has been described in detail.[14]

(15) Bortz, A. B.; Kalos, M. H.; Lebowitz, J. L. *J. Comput. Phys.* **1975**, *17*, 10–18.

From the above description of Monte Carlo algorithms, it is clear that the configuration of the lattice gas evolves stochastically in a simulation. If we consider the probability density in configuration space, the resulting time evolution for the stochastic process is described by the master equation[1,2]

$$dP(c_f,t)/dt = \sum_{c_i}\omega(c_i,c_f)P(c_i,t)/\tau - \sum_{c_i}\omega(c_f,c_i)P(c_f,t)/\tau \quad (1)$$

where $P(c,t)$ is the probability distribution of configuration c at time t. The transition probabilities $\omega(c_i,c_f)$, which are the input parameters in a Monte Carlo simulation, are determined by the microscopic properties of the system being simulated. All processes which occur on a time scale much shorter than τ are accounted for by these transition probabilities. For instance, in the case of surface diffusion, the vibrational motion resulting from the frustrated translation, parallel to the surface, of the molecule in the adsorption well determines the rate of escape from one adsorption site to the next. Hence, the transition probabilities for the surface diffusion simulation must correctly account for these underlying microscopic dynamics.

Since the particular stochastic process that results in the simulation is determined by the choice of the transition probabilities $\omega(c_i,c_f)$, it is important that this choice be made carefully. The transition probabilities $\omega(c_i,c_f)$ must at least satisfy detailed balance, i.e.,

$$\omega(c_i,c_f)P_{eq}(c_i) = \omega(c_f,c_i)P_{eq}(c_f) \quad (2)$$

This is necessary in order that the dynamics produce the correct equilibrium probability distribution $P_{eq}(c)$ in configuration space. This probability distribution is given by

$$P_{eq}(c) = Z^{-1}\exp(-H[c]/k_BT) \quad (3)$$

where H is the Hamiltonian and Z is the partition function. The requirement of detailed balance, however, does not completely specify the transition probabilities. It can be seen from eq 2 that detailed balance can only specify, for each pair c_i and c_f of configurations, the ratio $\omega(c_i,c_f)/\omega(c_f,c_i)$. If, for instance, we multiply each pair of transition probabilities $\omega(c_i,c_f)$ and $\omega(c_f,c_i)$ by a constant factor (which need not be the same for different transition pairs), we will obtain another system that has exactly the same equilibrium properties but different kinetics. One systematic way of doing this is by normalizing the transition probability $\omega(c_i,c_f)$ by the sum $\omega(c_i,c_f) + \omega(c_f,c_i)$ to obtain the transition probability

$$\tilde{\omega}(c_i,c_f) = \omega(c_i,c_f)/[\omega(c_i,c_f) + \omega(c_f,c_i)] \quad (4)$$

Similarly, we can define an $\tilde{\omega}(c_f,c_i)$ for the reverse transition. Using these rescaled transition probabilities in a simulation will give the same equilibrium distribution of configurations as a simulation using the original transition probabilities. However, the approach to equilibrium occurs at a different rate. Adsorption and desorption rate coefficients or diffusion rate coefficients obtained from simulations using $\tilde{\omega}(c_i,c_f)$ would be quite different from the corresponding quantities obtained from simulations using $\omega(c_i,c_f)$. Indeed, it is not simply the case that equilibrium is reached at a different rate. The two systems would proceed toward equilibrium along different ensembles of trajectories in configuration space.[13]

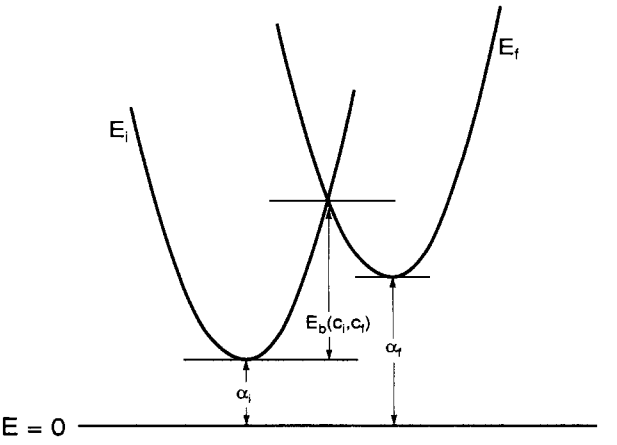

Figure 1. A schematic diagram of the model for the energy barrier for diffusion. The parameters α_i, α_f, and E_b which appear in eqs 5–7 are indicated explicitly.

Applications

Surface Diffusion. We now illustrate the ideas discussed above using the results of a previously reported[13] simulation of surface diffusion. The simulation system consists of a square lattice gas in which the nearest-neighbor and next-nearest-neighbor repulsions are of equal strength, ϕ. Surface diffusion is simulated for two different dynamic models, i.e., using two different sets of transition probabilities.

In the first dynamic model, which we will refer to as the thermal excitation model, the energy barrier $E_b(c_i,c_f)$ for a particle to hop to a nearest-neighbor site is obtained by computing the intersection of two parabolic potential wells described by

$$E_i = k\zeta^2/2 + \alpha_i \quad (5)$$

and

$$E_f = k(\zeta - \lambda)^2/2 + \alpha_f \quad (6)$$

Here E_i and E_f are the potential wells of the initial and final states, respectively, and ζ is the surface diffusion coordinate, as may be seen in Figure 1. The bottom of the initial potential well is given by $\alpha_i = \phi N_i$, where N_i is the total number of occupied sites that are nearest neighbor and next-nearest neighbor to the particle. Similarly, the bottom of the final potential well is computed by considering the neighborhood of the particle if it were in the final site. The lattice constant is λ, and the force constant of the (harmonic) potential wells is k. The energy barrier E_b to hop is given by the difference in energy between the point of intersection of the two potential wells and the bottom of the initial potential well. The transition probabilities are given by

$$\omega_e(c_i,c_f) = \exp[-E_b(c_i,c_f)/k_BT] \quad (7)$$

We choose $\lambda = 3$ Å and $\phi = 2$ kcal/mol. If the mass of the particle is chosen to be 10 amu, then the frustrated translational frequency parallel to the surface is equal to approximately 72 cm^{-1}. These values are typical of a number of adatoms on transition metal surfaces.

In the second dynamic model, the (Kawasaki) transition probabilities are given by

$$\omega_k(c_i,c_f) = \exp(-\delta\alpha/2k_BT)/[\exp(-\delta\alpha/2k_BT) + \exp(\delta\alpha/2k_BT)] \quad (8)$$

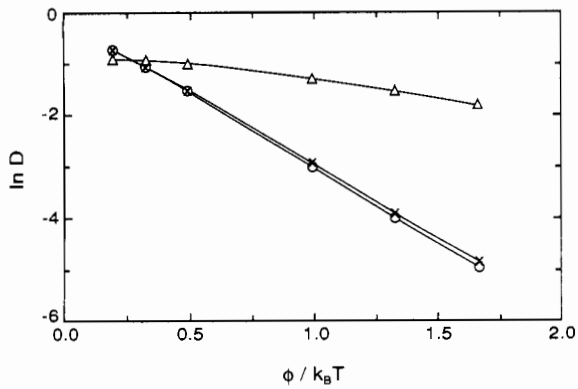

Figure 2. The dependence of the diffusion coefficient D (in units of λ^2/τ) upon reciprocal temperature $1/T$. The circles are results from simulations using the transition probabilities ω_e, the triangles are results from simulations using ω_k, and the crosses are results from simulations in which ω_k have been rescaled, as explained in the text.

where $\delta\alpha = \alpha_f - \alpha_i$. For each pair of configurations c_i and c_f, $\omega_e(c_i,c_f)$ and $\omega_k(c_i,c_f)$ are related by

$$\omega_k(c_i,c_f) = A(c_i,c_f)\omega_e(c_i,c_f) \tag{9}$$

where

$$A = \{\exp[(\delta\alpha/2k_BT) + (|\epsilon|/k_BT)]\}/[\exp(\delta\alpha/2k_BT) + \exp(-\delta\alpha/2k_BT)] \tag{10}$$

and $\epsilon = E_b - \delta\alpha$. It is easy to show that

$$\omega_k(c_i,c_f) = \omega_e(c_i,c_f)/[\omega_e(c_i,c_f) + \omega_e(c_f,c_i)] \tag{11}$$

(cf. eq 4). Therefore, the transition probabilities in the second model are simply the transition probabilities in the first model rescaled such that their sum for each pair of transitions $c_i \leftrightarrow c_f$ is equal to unity, i.e., the transition probabilities $\omega_e(c_i,c_f)$ and $\omega_k(c_i,c_f)$ are related in the same manner as the transition probabilites $\omega(c_i,c_f)$ and $\tilde{\omega}(c_i,c_f)$ discussed in the previous section. Therefore, it is expected that these two systems evolve toward the same equilibrium distribution of configurations but with different kinetics. We shall explain below the details of how this comes about.

Simulations were performed on 100×100 lattices of one-half fractional coverage at temperatures given by $0.6\phi/k_B \le T \le 5\phi/k_B$. The temperatures are sufficiently high that effects on diffusion due to the order–disorder transition,[16] with a critical temperature equal to $0.525\phi/k_B$, are not observed. In Figure 2 we plot the diffusion coefficients, in units of λ^2/τ, as a function of reciprocal temperature for the two dynamic models. The circles are results for the first model [using $\omega_e(c_i,c_f)$], and the triangles are results for the second model [using $\omega_k(c_i,c_f)$]. The diffusion barrier for the first model varies from approximately 2.6ϕ at high temperatures to approximately 3.0ϕ at low temperatures. At lower temperatures the probability of finding local configurations that are energetically more favorable, and hence have a higher diffusion barrier, becomes higher. Thus, a higher diffusion barrier is expected at lower temperatures. At infinite temperature the average neighborhood of a particle before and after hopping is the same. For our lattice-gas model, this implies a lower limit of 2.5ϕ for the diffusion barrier when thermal excitation dynamics are used. For Kawasaki dynamics the same

(16) Sadiq, A.; Binder, K. *Surf. Sci.* **1983**, *128*, 350–382.

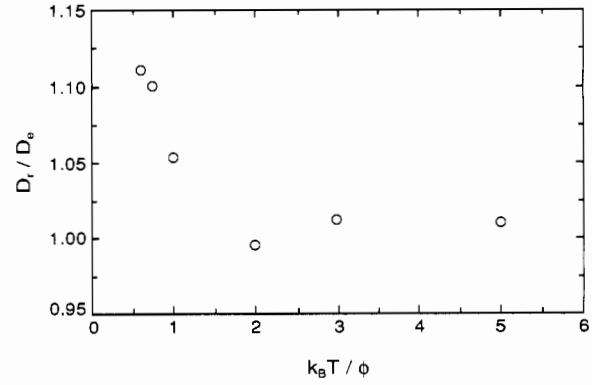

Figure 3. The ratio D_r/D_e of the diffusion coefficients plotted in Figure 2. This clearly shows that the ratio deviates from unity at low temperatures.

argument shows that at infinite temperature the diffusion barrier is 0. This is confirmed by the simulation results which show a decrease in the diffusion barrier toward 0 at the higher temperatures when using these dynamics (cf. Figure 2).

For the thermal excitation model, the slope of the corresponding curve in Figure 2 is conventionally interpreted as the energy barrier to surface diffusion. For Kawasaki dynamics the slope of the Arrhenius construction in Figure 2 can, *at best*, be taken as an effective energy barrier. The interpretation of the slope as an energy barrier is not entirely satisfactory because, independent of the lattice-gas model, Kawasaki dynamics will always give a diffusion barrier which tends to 0 at high temperatures.

These results illustrate two points. First, the computed diffusion coefficients are different for models with different transition probabilities, even though the equilibrium states are equivalent. Second, this difference is not a trivial temperature-independent rescaling, because the temperature dependence of the diffusion coefficients is not the same. In order to emphasize this latter point, we can rescale the time in the simulations in an attempt to make the diffusion coefficients agree. Using eq 9, we can divide the time increment for each step in the second model by the appropriate $A(c_i,c_f)$. The results of such a procedure are shown as crosses in Figure 2. The ratio of the diffusion coefficient D_r obtained in this way to that obtained in the first model is plotted in Figure 3. The agreement between D_r and D_e is good for temperatures that are high compared to ϕ/k_B. The agreement becomes progressively poorer as the temperature becomes progressively lower. This is easily understood as follows. At high temperatures the factor $A(c_i,c_f)$ is weakly dependent on the configurations c_i and c_f since the distribution of configurations is rather uniform. Therefore, all the transition probabilities $\omega_e(c_i,c_f)$ are rescaled by approximately the same factor to get $\omega_k(c_i,c_f)$. This means that the relative probability of picking a transition is approximately the same for both dynamic models. At lower temperatures, however, $A(c_i,c_f)$ becomes strongly dependent upon the configurations c_i and c_f. This results in different relative probabilities for picking a transition in the two dynamic models. Thus, in each dynamic model the system evolves along a different ensemble of trajectories in configuration space. In both cases the system evolves toward the same equilibrium state, but the paths taken in getting there are different. In the case in which there

are no lateral interactions, however, the two sets of transition probabilities would yield equivalent results.

The thermal excitation model is appropriate for describing systems in which the probability of escape from one adsorption well into another has the form $\nu \exp(-E/k_BT)$, where E is an energy barrier. For these systems the Kawasaki model is simply not appropriate. When the thermal excitation model is used, the potential wells must be prescribed in order to calculate the energy barrier. This difference, i.e., the presence of an energy barrier in the thermal excitation dynamics and the absence of one in Kawasaki dynamics, results in a rather fundamental difference between the two dynamics.

In order to amplify this important point, consider a δ-function population distribution in configuration space with an initial configuration c_0. (This, of course, is the situation in any particular run of a Monte Carlo simulation.) Let the set of all configurations that can be reached from c_0 after one transition be C_0. After time τ, one attempt at a transition has occurred, and the region of configuration space which can possibly be occupied is $(c_0 + C_0)$. If we use Kawasaki dynamics, it can be seen from eq 8 that the population in the configurations $(c_0 + C_0)$ is now distributed according to the Boltzmann distribution. Of course, the system is not in thermal equilibrium because there are unpopulated configurations that are accessible only after more than one transition has occurred. On the other hand, if we use thermal excitation dynamics, the population in the configurations $(c_0 + C_0)$ becomes Boltzmann distributed only after many attempts at transitions between these configurations have occurred. The number of attempts needed is expected to be proportional to $\exp(E/k_BT)$, where E is the largest energy barrier for the transitions among the configurations $(c_0 + C_0)$.

We should also note that other forms of the transition probability $\omega(c_i,c_f)$ have been used previously.[3-13] In one of these proposed alternatives,[6] the transitions are sampled according to Kawasaki dynamics, but the unit of time τ is taken to be $\tau_0 \exp(E/k_BT)$, where τ_0 is a constant. In this case, E is the energy barrier, and τ becomes temperature dependent rather than a constant. In a sense, this is similar to thermal excitation dynamics, because the population of the configuration in the set $(c_0 + C_0)$ becomes Boltzmann distributed after a time inversely proportional to the Boltzmann factor for an energy barrier.

The Compensation Effect. An interesting phenomenon that Monte Carlo simulations have been used to investigate is the compensation effect seen in many surface chemical reactions. This effect, which involves a compensation between variations in the preexponential factor and the activation energy of the reaction rate coefficient, has been observed for many systems involving both unimolecular and bimolecular reactions on solid surfaces. The activation energy is expected to vary with the fractional surface coverage because of lateral interactions between the adsorbed molecules. In compensating systems the apparent preexponential factor also varies with the fractional coverage such that as the activation energy increases, the preexponential factor also increases, resulting in a compensation in the observed rate. Although changes in the activation energy can be understood microscopically in terms of adsorbate–adsorbate interactions, the concomitant changes in the preexponential factor are poorly understood. A recent review[17] correctly stated that current theories cannot account for the frequently very large (up to 11 orders of magnitude[18]) range of variation of the preexponential factor. Changes in the surface phonon spectrum may play a role in the compensation effect, but the theories that take this into account have heretofore dealt only with low fractional coverages.[19-21] Our recent work[22,23] shows that the parametrization implicit in the Polanyi–Wigner form of the reaction rate coefficient, $k_r = k^{(0)} \exp(-E/k_BT)$, can lead to compensatory behavior when the local configuration of the adsorbate around a pair of reacting molecules changes with temperature. We studied the case of a bimolecular reaction between two lattice gases which were chosen to model the oxidation of carbon monoxide on single-crystalline transition metal surfaces.

This lattice-gas system can be described by the reactions

$$A_2(g) + 2v \rightleftharpoons 2A(s)$$

$$B(g) + v \rightleftharpoons B(s)$$

$$A(s) + B(s) \rightleftharpoons AB(g) + 2v$$

where (g) denotes a gas-phase molecule, (s) denotes an adsorbed species, v denotes a vacant adsorption site, and 2v denotes a pair of nearest-neighbor vacant adsorption sites.[22] We used a square lattice of adsorption sites to model the surface and assumed the occurrence of only nearest-neighbor interactions.

In the model we set the adsorption and desorption of B to be much faster than both the surface diffusion of A and the bimolecular reaction. This was done in order to simulate the relatively facile adsorption–desorption equilibrium of carbon monoxide compared both to its oxidation and to the surface diffusion of chemisorbed oxygen atoms. Hence, at each step in the simulations, the surface configuration of B is allowed to relax fully. This was done by using a Langmuir-like adsorption isotherm to compute the probability of finding an adsorbed B molecule at each vacant site on the surface. For a vacant site with j nearest-neighbor A's, this probability is equal to

$$P_{B,j} = [1 + \alpha \exp(-E_{d,j}/k_BT)]^{-1} \quad (12)$$

where

$$\alpha = k_d^{(0)}(2\pi m_B k_B T)^{1/2}/p_{B,g}A \quad (13)$$

and

$$E_{d,j} = E_{d,0} - j\epsilon_{AB} - (4 - j)P_{B,0}\epsilon_{BB} \quad (14)$$

The partial pressure of B in the gas phase is given by $p_{B,g}$, ϵ_{ij} are the nearest-neighbor interaction energies

(17) Seebauer, E. G.; Kong, A. C. F.; Schmidt, L. D. *Surf. Sci.* **1988**, *193*, 417–436.
(18) Engstrom, J. R.; Weinberg, W. H. *Surf. Sci.* **1988**, *201*, 145–170.
(19) Carter, K. F. *Surf. Sci.* **1983**, *125*, 499–514.
(20) Armand, G.; Masri, P.; Dobrzynski, L. *J. Vac. Sci. Technol.* **1972**, *9*, 705–712.
(21) Hood, E.; Jedrzejek, C.; Freed, K. F.; Metiu, H. *J. Chem. Phys.* **1984**,*81*, 3277–3293.
(22) Kang, H. C.; Jachimowski, T. A.; Weinberg, W. H. *J. Chem. Phys.* **1990**, *93*, 1418–1429.
(23) Fichthorn, K. A.; Weinberg, W. H. *Langmuir* **1991**, *7*, 2539–2543.

between species i and j, A is the area of a unit cell which is taken to be 10^{-15} cm^2, and the rate coefficient for desorption of B is $k_d = k_d^{(0)} \exp(-E_{d,j}/k_BT)$.

The role of the Monte Carlo sampling is to simulate the microscopic events of dissociative adsorption, surface diffusion, and reaction of A. The dissociative adsorption rate on a pair of nearest-neighbor sites i and j, which are unoccupied by A, is given by

$$r_a(i,j) = (1 - P_{B,i})(1 - P_{B,j})p_{A_2}A/(2\pi m_{A_2}k_BT)^{1/2} \quad (15)$$

where p_{A_2} is the partial pressure of gas-phase A_2 and m_{A_2} is the molecular mass of A_2. The probabilities $P_{B,i}$ and $P_{B,j}$ account for the possible occupation of each of the sites i and j by a B molecule.

The rate of hopping of a chemisorbed A atom from site i to a nearest-neighbor site j unoccupied by A is given by

$$r_h(i,j) = \nu_\parallel \exp[-E_h(i,j)/k_BT](1 - P_{B,j}) \quad (16)$$

where $\nu_\parallel$ is the frustrated translational frequency of an A adatom parallel to the surface and $E_h(i,j)$ is the energy barrier to thermally activated diffusion. This barrier is obtained in the same manner as discussed earlier in connection with surface diffusion, i.e., the potential wells at sites i and j are modeled by two harmonic wells, and the top of the diffusion barrier is the intersection of these two wells (cf. Figure 1).

Given that an A atom is adsorbed at site i, the rate of reaction of this atom is given by

$$r_r(i,j) = 2k_r^{(0)} \exp[-E_r(i,j)/k_BT]P_{B,j} \quad (17)$$

where the factor $P_{B,j}$ accounts for the probability of finding a B in the neighboring site j, and $k_r^{(0)}$ is the preexponential factor of the reaction rate coefficient. The activation energy $E_r(i,j)$ is computed via

$$E_r(i,j) = E_{r,0} - n_{AA}\epsilon_{AA} - n_{BB}\epsilon_{BB} - (n_{AB}\epsilon_{AB} + n_{BA}\epsilon_{BA}) \quad (18)$$

Here, n_{AA} and n_{BA} are the numbers of nearest-neighbor A and B species, respectively, to the A atom in the reacting pair, and n_{BB} and n_{AB} are the numbers of nearest-neighbor B and A species, respectively, to the B particle in the reacting pair. The ϵ's are the magnitudes of the corresponding interaction energies (positive if repulsive), and $\epsilon_{BA} = \epsilon_{AB}$. The activation energy of reaction of an isolated AB pair is given by $E_{r,0}$.

All the parameters in the above expressions for the rates of diffusion, adsorption, and reaction of A and for the Langmuir isotherm describing the configuration of B are chosen such that the reaction between oxygen and carbon monoxide on platinum[18] is simulated. The chosen values of the various parameters have been given previously.[22,23] It is essential to note here only that the preexponential factors in the above expressions are constants, i.e., no variation with coverage or temperature is built into the model. The results of these simulations, in which the temperature ranged from 325 to 500 K and the gas-phase partial pressure of B was maintained at 10^{-6} Torr, are shown in Figure 4. The activation energy and the preexponential factor of the reaction rate coefficient are plotted as a function of the gas-phase pressure of A_2. There is clearly a large (7 orders of magnitude) variation in the preexponential factor, and this variation compensates for the variation in the activation energy.

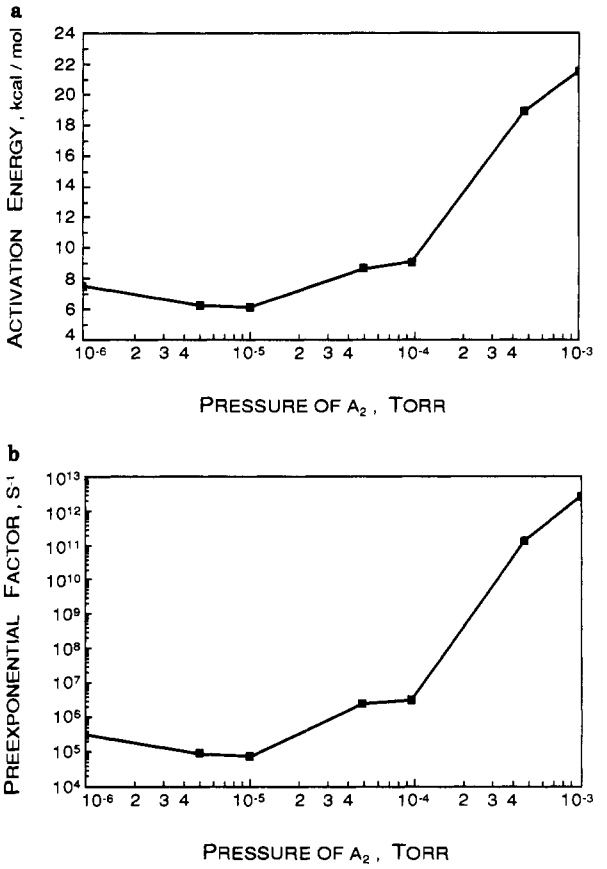

Figure 4. (a) The activation energy of the reaction rate coefficient as a function of the gas-phase pressure of A_2. The gas-phase pressure of B is 10^{-6} Torr throughout, and the temperature ranged from 325 to 500 K. (b) The preexponential factor of the reaction rate coefficient as a function of the gas-phase pressure of A_2, for the same set of simulations as in Figure 4a.

Previously, we modeled a similar system,[22] except that no diffusion of the adsorbed A was allowed, and no lateral interactions occurred between B particles. In that study a few different values for the interaction ϵ_{AB} between adsorbed A and B particles were used. The compensation effect was observed when the distribution of local configurations of an AB pair depended significantly upon temperature. When this strong temperature dependence was not observed, the compensatory trend was either absent or weak. More detailed results, in particular the change in the distribution of local configurations with temperature, can be found elsewhere.[22,23] Initially, we studied systems which were not at steady state, and we computed only the initial reaction rate as a preadsorbed overlayer of A particles was exposed to B.[22] However, we argued there that the observation of a compensation effect is not affected by the transient nature of the simulations. In particular, the fact that the coverage is not a constant[24] does not affect the conclusions presented there. This was confirmed subsequently[23] when steady-state systems were simulated.

In all the systems that we have simulated,[22,23] the observed compensation effect can be related to the dependence on temperature and fractional coverage of the distribution of local configurations. Now we shall briefly summarize the framework within which the results can be understood. This will also underscore the

(24) Zhdanov, V. P. *Surf. Sci. Rep.* **1991**, *12*, 184–242.

usefulness of Monte Carlo simulations for situations in which the configuration of particles in the system (here the configuration of the adsorbed overlayer) varies in a nontrivial fashion.

The usual analysis of bimolecular Langmuir–Hinshelwood reactions assumes that the reaction rate is given by

$$R = k_r\theta_A\theta_B = k^{(0)} \exp(-E/k_BT)\theta_A\theta_B \qquad (19)$$

where the rate coefficient k_r is assumed to be of the Polanyi–Wigner form with the possibility of a temperature- and coverage-dependent activation energy E and preexponential factor $k^{(0)}$. It is also possible to consider the reaction rate to be the sum over the distribution $\theta_{AB,i}$ of reactant pairs whose local environment, through adsorbate interactions, dictates an activation energy E_i and a preexponential factor $k_i^{(0)}$, i.e.,

$$R = \sum_i \theta_{AB,i} k_i^{(0)} \exp(-E_i/k_BT) \qquad (20)$$

In the simulation we set all the $k_i^{(0)}$'s to be equal. A similar expression was suggested many years ago to account for compensation in terms of the intrinsic heterogeneity of a catalyst in the absence of adsorbate interactions.[25] By comparison of the above two expressions, eqs 19 and 20, for the reaction rate, it can be seen that each of the two parameters E and $k^{(0)}$ in eq 19 is a weighted average depending on all the microscopic $k_i^{(0)}$'s and E_i's in eq 20. Hence, the variation in the distribution of reactant pairs, $\theta_{AB,i}$ which accompanies temperature or fractional coverage changes will vary the contribution of each $k_i^{(0)}$ and each E_i toward $k^{(0)}$ and E. Clearly, temperature or coverage changes can result in variations in the apparent preexponential factor $k^{(0)}$ and the apparent activation energy E in eq 19.

A conventional way of presenting the compensation effect is the variation of $k^{(0)}$ and E with temperature at a constant coverage. If we consider eq 20, it can be seen that the total reaction rate is the average over all local configurations of the reaction rate $k_i^{(0)} \exp(-E_i/k_BT)$ for each type of local configuration, each one of which is weighted by its corresponding factor $\theta_{AB,i}$. The $\theta_{AB,i}$ factors give the distribution of AB pairs in each type of local configuration. As the temperature is lowered, while a constant coverage is maintained, the probability of finding AB pairs in energetically favorable local configurations increases. Thus, $\theta_{AB,i}$ for local configurations with high activation energy E_i increases at the expense of $\theta_{AB,i}$ for local configurations with low activation energy E_i. Consequently, in an Arrhenius plot of the reaction rate R, the logarithm of R is a concave function of $1/T$. Therefore, we conclude that a compensation effect (as opposed to an anticompensation effect) will generally be observed.

It should be emphasized that although it is relatively simple to make qualitative arguments for the occurrence of compensatory trends, it is not an altogether trivial task to obtain quantitative support for these arguments. Unless the variations in $\theta_{AB,i}$ (which is a nearest-neighbor correlation) with temperature and coverage are well approximated by mean-field theories, and can therefore be easily computed, it is necessary to use Monte Carlo sampling in order to compute $\theta_{AB,i}$.

(25) Constable, F. H. *Proc. R. Soc. London, A* **1925**, *108*, 355.

Conclusions

We have discussed the basis for using Monte Carlo simulations to study dynamic phenomena. The correspondence between a Monte Carlo step and an increment in real time can be quantified using the theory of Poisson processes. We have shown that the transition probabilities $\omega(c_i,c_f)$ describing the system play a central role in determining the real-time increment for each step in a simulation. In particular, the real-time increment corresponding to a step in a simulation is equal to the reciprocal of $\langle\langle \omega(c_i,c_f)/\tau \rangle\rangle$. Here the ensemble average $\langle\langle\ \rangle\rangle$ is over all trajectories for each initial configuration and over a distribution of initial configurations consistent with some specified macroscopic parameters.

The appropriate choice of transition probabilities is important because it is possible to have systems, described by different sets of transition probabilities, which take different (ensemble averaged) paths toward equilibrium, even though the equilibrium distribution of configurations is the same. We illustrated by discussing the use of dynamic Monte Carlo simulations to study the surface diffusion of a lattice gas. Two dynamic models sharing the same equilibrium distribution of configurations but having different transition probabilities, $\omega(c_i,c_f)$, were studied. A difference in the temperature dependence of the surface diffusion coefficient for these systems was observed. This difference became increasingly significant at lower temperatures because of the increasingly different ensembles of trajectories taken in evolving toward equilibrium.

We also discussed the use of dynamic Monte Carlo simulations to study the compensation effect in a Langmuir–Hinshelwood reaction. A lattice-gas system simulating the reaction between carbon monoxide and oxygen on transition metal surfaces was studied. The use of Monte Carlo simulations here was essential because it allowed us to show that a possible origin of the compensation effect is in the variation, with temperature and fractional surface coverage, of the adlayer configuration. Monte Carlo simulations make it possible to generate the nontrivial variation of the adlayer configurations. This application demonstrates the usefulness of dynamic Monte Carlo simulations in providing microscopic insight for understanding some macroscopic features of complicated reaction systems.

We gratefully acknowledge the financial support of the Department of Energy (Grant DE-FG03-89ER14018), the National Science Foundation (Grant CHE-9003553), and the donors of the Petroleum Research Fund, administered by the American Chemical Society (Grant 23801-AC5-C). We also appreciate numerous helpful discussions with Professor Kristen A. Fichthorn.